



## Research Article

# Sensitivity Analysis and Optimal Control of Cocoa Black Pod Disease Caused by *Phytophthora Margakarya*

Adebayo Adeniran<sup>1,3\*</sup> , Adeniyi Onanaye<sup>1</sup>, Olawale Adeleke<sup>1</sup>, Mathew Odekunle<sup>2</sup>

<sup>1</sup>Department of Mathematics and Statistics, Redeemer's University, Ede, Nigeria

<sup>2</sup>Department of Mathematics, Modibbo Adama University, Yola, Nigeria

<sup>3</sup>Department of General Studies, Federal Polytechnic, Ile-Oluji, Nigeria

E-mail: adeniran9867@run.edu.ng

**Received:** 22 December 2023; **Revised:** 25 April 2024; **Accepted:** 25 April 2024

**Abstract:** To address the critical threat black pod disease poses to global cocoa production and farmer income, this study developed a novel mathematical model that utilizes a system of ordinary differential equations to capture the interactions between various stages of cocoa pods (susceptible cherelles, young/mature pods, ripe pods) and their disease state (exposed, infected). Additionally, the model incorporates the dynamics of the disease-causing pathogen population. Employing Pontryagin's Maximum Principle, the model optimizes control strategies that minimize disease impact. This optimization identifies the efficient allocation of resources, timing of interventions, and deployment of control measures like infected pod removal, fungicides, and sanitation practices. The finding of the study reveals that control measure  $u_3$  which is rouging (pod removal) and any one of the remaining control measures is best for the treatment of cocoa black pod disease caused by *Phytophthora Megarkaya*. These findings translate into valuable, data-driven recommendations for cocoa farmers and disease management professionals. By strategically combining infected pod removal, targeted fungicide use, and environmental management practices, farmers can significantly reduce disease severity, enhance cocoa production, and promote a more sustainable cocoa industry.

**Keywords:** cocoa, dynamics, basic reproductive number, optimal control, pontryagin's maximum principle

**MSC:** 92xx, 91-10

## 1. Introduction

Infectious diseases have plagued humanity throughout history, leaving trails of devastation and shaping the course of civilizations. To understand and effectively combat these invisible foes, we turn to the power of mathematics. Mathematical models, intricate tapestries woven from data and equations, offer a unique lens through which we can observe the dance of infection within populations. By dissecting the dynamics of transmission, recovery, and immunity, these models provide invaluable insights for public health interventions, vaccination strategies, and outbreak control [1–4].

Cocoa, the source of our cherished chocolate, stands threatened by a silent enemy: black pod disease, caused by the fungal pathogen *Phytophthora palmivora* and *Phytophthora megakarya* [5], is a major threat to cocoa production

worldwide. It can cause devastating losses, leading to significant economic hardship for farmers and impacting the global chocolate supply chain [5, 6].

The fungus infects all parts of the cocoa tree, but the pods are most susceptible, particularly during periods of high humidity and rainfall [4, 6]. Spores spread through rain splashes, landing on pods and initiating infection. Initially, small, brown spots appear, rapidly growing to cover the entire pod surface. Infected pods turn black and mummified, with the cocoa beans inside rotting and becoming unusable [7].

Black pod disease can cause yield losses of up to 30% annually, with some regions experiencing even higher losses if fungicide use is limited [4, 7, 8]. This not only impacts farmers' livelihoods but also disrupts the global cocoa market, potentially leading to price fluctuations for chocolate consumers.

West Africa, the world's leading cocoa producer, faces a significant threat from black pod rot caused primarily by the fungus *Phytophthora megakarya*. This devastating disease rots cocoa pods, crippling yields and jeopardizing the livelihoods of millions of farmers [4–6].

*Phytophthora megakarya*'s primary host is the *Theobroma cacao* tree. It is the most virulent species of *Phytophthora* that infects cocoa, causing the greatest percentage of yield loss. The disease it causes is called black pod rot, its symptoms are root rot on seedlings, cankers on stems and branches, black and rotting pods [5, 6]. *P. megakarya* reproduces through motile spores called zoospores. These zoospores are released from infected pods and can travel in water to find new hosts, once they reach a cocoa tree, the zoospores encyst and germinate, producing a germ tube that penetrates the host tissue [5].

Inside the host, the oomycete grows and spreads, feeding on the plant's cells. Which lead to the infected pods becoming black and rotten. The disease thrives under warm and humid conditions, heavy rainfall and poor drainage can favor the spread of the disease. There is no single cure for black pod rot. but an integrated approach using cultural, chemical, and biological control methods is often necessary [4–6].

Plant diseases pose a significant threat to global food security, causing billions of dollars in losses annually [9]. To effectively manage and mitigate these diseases, researchers are increasingly turning to mathematical modeling. These models provide a quantitative framework for understanding disease dynamics, predicting outbreaks, and evaluating the effectiveness of control strategies. A common approach utilizes compartmental models, which categorize plant populations into distinct stages based on their disease status. For example, a black pod disease model might have compartments for susceptible pods, infected pods, and recovered pods [7]. Systems of ordinary differential equations then describe the transition rates between these compartments, often incorporating factors like weather conditions, pathogen dispersal, and control measures.

Recent research in mathematical modeling of infectious plant diseases has seen several advancements:

- **Spatially Explicit Models:** These models incorporate spatial information to capture the geographical spread of disease across fields or regions. This allows for a more realistic representation of disease dynamics, particularly for wind-dispersed pathogens [10].

- **Age-Structured Models:** These models consider the age or developmental stage of plants, as susceptibility to disease can vary depending on this factor [11].

- **Stochastic Models:** These models account for the inherent randomness in disease transmission, providing a more probabilistic picture of disease progression [12].

Mathematical models offer several benefits in plant disease management:

- **Predicting Outbreaks:** Models can be used to predict the timing and severity of potential outbreaks, allowing for proactive implementation of control measures [12].

- **Optimizing Control Strategies:** By simulating different control strategies within the model, researchers can identify the most effective and resource-efficient approach for a specific disease scenario [13].

- **Evaluating New Technologies:** Models can be used to assess the potential impact of new disease control technologies before their widespread adoption [12].

Mathematical modeling transcends mere observation by venturing into the realm of optimal control theory. This framework leverages the insights gained from models to identify the most effective strategies for disease management. [14, 15] employed dynamic programming to optimize fungicide application in black pod control, demonstrating significant

yield improvements compared to static schedules, this work highlighted the potential of tailoring interventions to the specific dynamics of each outbreak. Optimal control theory allows researchers to determine the most effective allocation of resources and timing of interventions for disease control. Techniques like Pontryagin's Maximum Principles are employed to identify control strategies that minimize disease impact or maximize yield [16, 17].

The foundation of mathematical modeling in cocoa disease lies in compartmental models. These frameworks divide the cocoa population into distinct compartments, often representing susceptible pods, infected pods, and recovered (resistant) pods. The flow of pods between these compartments is governed by a set of equations, incorporating parameters like transmission rates due to fungal spores or viral vectors, recovery times, and potential interventions [8, 18–20].

Early work by [19] established a basic framework for modeling black pod disease, a fungal like scourge responsible for significant losses. Their model effectively captured the disease's exponential growth and provided insights into the impact of sanitation practices. [21] further refined this approach by modeling the spread of cacao swollen shoot virus (CSSV), highlighting the crucial role of vector movement and host susceptibility.

Beyond fungicides, [22] provided a comprehensive review of optimal control approaches in plant disease management, encompassing strategies like varietal selection, intercropping, and sanitation, this review emphasized the need for flexible models that can incorporate diverse control options and adapt to changing environmental conditions.

Mathematical models and optimal control theory hold immense potential for revolutionizing cocoa disease management. By providing insights into disease dynamics and optimizing interventions, these tools can empower farmers to protect their crops, secure their livelihoods, and ensure the continued flow of chocolate for generations to come. Addressing the existing challenges and fostering continued research in this field are crucial steps towards a future where cocoa thrives, disease is contained, and the sweet symphony of chocolate continues to delight the world [15, 23].

## 2. Model formulation

The total pod population at time  $t$ , represented by  $N(t)$  is subdivided into six compartments of Cherelles  $S_c(t)$  (flowering and formation of young pod stage); young and Mature pod stage  $S_m(t)$ ; Ripe pod  $S_r(t)$ ; exposed  $E(t)$  (pod that are infected but cannot transmit the infection); Infected pods  $I(t)$  (pod that are infected and infectious); Removed pods  $R(t)$  (infected ripe pods but are of economic importance and healthy ripe pods that are harvested). Then

$$N(t) = S_c(t) + S_p(t) + S_r(t) + E(t) + I(t) + R(t). \quad (1)$$

The total pathogen population is denoted by  $N_p(t)$  and it consist of only one compartment, i.e  $N_p(t) = P(t)$ .

Compartment  $S_c(t)$  and  $S_m(t)$  are exposed to pod infection whenever there is any form of interaction with the Pathogen of infection  $P(t)$ , the transmission mode of *Phytophthora Margakaya* may be through rain splash, direct contact, infected plant material, insects, equipment and environmental factors such as warm, humid weather, poor drainage and densely planted trees.

Figure 1 describe the transmission of the disease from the environment to the healthy pod compartment.

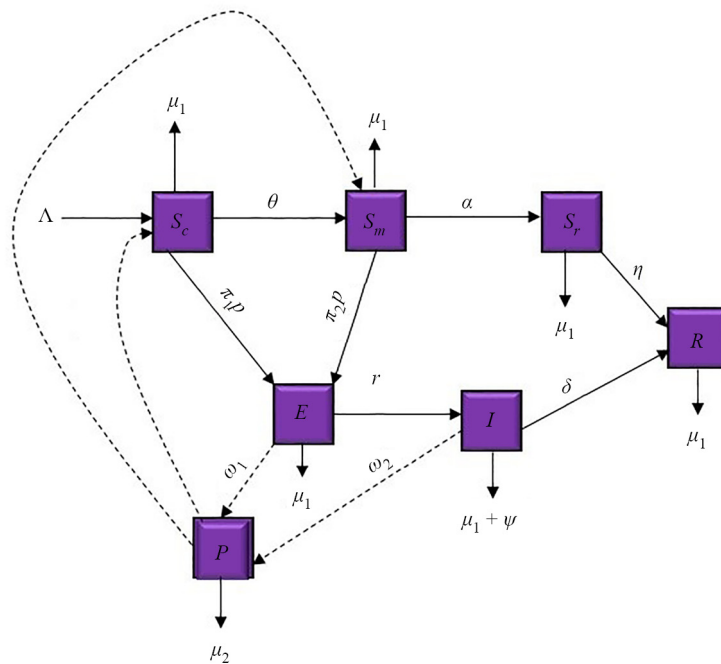


Figure 1. Flow diagram showing of the model

From the description of model parameters in Table 1 and the compartmental diagram in Figure 1, we have the following system of differential equation.

$$\left. \begin{aligned}
 \frac{dS_c}{dt} &= \Lambda - \pi_1 P S_c - (\theta + \mu_1) S_c, \\
 \frac{dS_m}{dt} &= \theta S_c - (\pi_2 P + \alpha + \mu_1) S_m, \\
 \frac{dS_r}{dt} &= \alpha S_m - (\mu_1 + \eta) S_r, \\
 \frac{dE}{dt} &= (\pi_1 S_c + \pi_2 S_m) P - (\omega_1 + \gamma + \mu_1) E, \\
 \frac{dI}{dt} &= \gamma E - (\delta + \mu_1 + \psi) I, \\
 \frac{dR}{dt} &= \delta I + \eta S_r - \mu_1 R, \\
 \frac{dP}{dt} &= \omega_1 E + \omega_2 I - \mu_2 P.
 \end{aligned} \right\} \quad (2)$$

$$(S_c(0), S_m(0), S_r(0), E(0), I(0), R(0), P(0)) \geq 0$$

**Table 1.** Description of model parameters and values

Parameter	Descriptions	value	Source
$S_c$	Cherelles compartment		
$S_m$	Young and Mature pod compartment		
$S_r$	Ripe pod compartment		
$E$	Exposed pod compartment		
$I$	Infected pod compartment		
$T$	Treated pod compartment		
$R$	Removed/ Harvested pod compartment		
$P$	Pathogen compartment		
$\Lambda$	Recruitment rate	12	[24, 25]
$\pi_1$	Transmission rate from $P(t)$ to $S_c(t)$	0.0007954551	[26]
$\alpha$	Transmission rate from $S_m$ to $S_r$	0.027	[26]
$\pi_2$	Transmission rate from $P(t)$ to $S_m(t)$	0.0007954551	[26]
$\theta$	Transmission rate from $S_c(t)$ to $S_m(t)$	0.05	[27]
$\mu_1$	Natural death rate	0.05	[27]
$\mu_2$	The decay rate of Pathogen in $P(t)$	0.00900982	[26]
$\alpha$	Ripening rate ( $S_m(t)$ to $S_r(t)$ )	0.027	[24]
$\eta$	Removed rate of either ripe or decay	0.09	[27]
$\omega_1$	Rate of increase from $P(t)$ to $E(t)$	0.0587364	[26]
$\omega_2$	Rate of increase from $P(t)$ to $I(t)$	0.0587364	[26]
$\gamma$	Progression rate of $E(t)$ to $I(t)$	0.01	[25, 27]
$\delta$	Transmission rate from $I$ to $R$	0.09	[25, 27]
$\psi$	Death rate as a result of the infection	0.0001	[26]

### 3. Model analysis

Analyzing epidemic models is crucial for understanding and predicting the spread of infectious diseases. These models, though simplified representations of reality, offer valuable insights into factors influencing disease dynamics and inform public health interventions.

#### 3.1 Boundedness of the model

**Lemma 1** Let the initial conditions of the system (2) be nonnegative in  $\mathfrak{R}_+^6 \times \mathfrak{R}_+^1$ ,

$$\Omega_N = \left\{ (S_c, S_m, S_r, E, I, R) \in \mathfrak{R}_+^6; N(t) \leq \frac{\Lambda}{\mu_1} \right\},$$

$$\Omega_P = \left\{ P \in \mathfrak{R}_+^1; P(t) \leq \frac{\Lambda(\omega_1 + \omega_2)}{\mu_1 \mu_2} \right\}, \quad (3)$$

then the set  $\Omega = \Omega_N \times \Omega_P$  is positively invariant.

**Proof.** The first six equation of system (2) will be added to obtain

$$\frac{dN}{dt} = \Lambda - \mu_1 N - \psi I, \quad (4)$$

in the absence of infection i.e  $I = 0$ , we have

$$\frac{dN}{dt} \leq \Lambda - \mu_1 N, \quad (5)$$

solving (5), yields

$$N(t) \leq \frac{\Lambda}{\mu_1} + \left( N(0) - \frac{\Lambda}{\mu_1} \right) e^{-\mu_1 t}, \quad (6)$$

as  $t \rightarrow \infty$

$$N(t) \leq \frac{\Lambda}{\mu_1}, \quad (7)$$

hence, the feasible solution region is given by

$$\Omega_N = \left\{ (S_c, S_m, S_r, E, I, R) \in \mathfrak{R}_+^6; N(t) \leq \frac{\Lambda}{\mu_1} \right\}.$$

Likewise, by considering the seventh equation of system (2), i.e.

$$\frac{dP}{dt} = \omega_1 E + \omega_2 I - \mu_2 P, \quad (8)$$

Rewriting (8) as

$$\frac{dP}{dt} \leq \frac{\Lambda(\omega_1 + \omega_2)}{\mu_1} - \mu_2 P, \quad (9)$$

on solving (9),

$$P(t) \leq \frac{\Lambda(\omega_1 + \omega_2)}{\mu_1 \mu_2} - \frac{1}{\mu_2} \left[ \frac{\Lambda(\omega_1 + \omega_2)}{\mu_1} - \mu_2 P(0) \right] e^{-\mu_2 t}, \quad (10)$$

as  $t \rightarrow \infty$

$$P(t) \leq \frac{\Lambda(\omega_1 + \omega_2)}{\mu_1 \mu_2}.$$

Hence

$$\Omega_P = \left\{ P \in \mathfrak{R}_+^1; P(t) \leq \frac{\Lambda(\omega_1 + \omega_2)}{\mu_1 \mu_2} \right\}.$$

Thus, the feasible region defined by the set

$$\Omega = \Omega_N \cup \Omega_P \subset \mathfrak{R}_+^6 \times \mathfrak{R}_+^1.$$

is positively invariant. □

### 3.2 Positivity of solutions

**Lemma 2** Let  $S_c(0), S_m(0), S_r(0), E(0), I(0), R(0), P(0)$  be the initial conditions of the system (2), then the solution of  $S_c, S_m, S_r, E, I, R, P$  are nonnegative  $\forall t > 0$ .

**Proof.** Considering the first equation of system (2)

$$\frac{dS_c}{dt} = \Lambda - \pi_1 P S_c - (\theta + \mu_1) S_c, \tag{11}$$

rearranging equation (11), we have

$$\frac{dS_c}{dt} + \pi_1 P S_c + (\theta + \mu_1) S_c = \Lambda, \tag{12}$$

on integrating (12) from 0 to  $T$ , we have

$$S_c(t) = \exp \left[ - \int_0^t (\pi_1 P + \theta + \mu_1) S_c dt \right] \left\{ S_c(0) + \int_0^t \Lambda \exp \left[ \int_0^t (\pi_1 P + \theta + \mu_1)(t) dt \right] dt \right\}. \tag{13}$$

Thus,  $S_c(t) \geq 0 \forall t > 0$ . In a similar approach, we prove the rest equations of equation (2).  $S_m(t) \geq 0, S_r(t) \geq 0, E(t) \geq 0, I(t) \geq 0, R(t) \geq 0, P(t) \geq 0$ , thus all the solutions are nonnegative  $\forall t > 0$ . □

### 3.3 Disease free equilibrium

A disease-free equilibrium (DFE) is a state in a disease transmission model where the number of infected individuals remain at zero over time. In other words, the disease dies out and disappears from the population. This concept is often used in mathematical models to study the dynamics of infectious diseases [28].

The key characteristics of a disease-free equilibrium are :

• No infected individuals: As mentioned earlier, the number of infected individuals in the population is zero at DFE. This means that the disease is not being transmitted and all individuals are either susceptible or recovered [28].

• Balance of rates: At DFE, the rate at which new infections occur is equal to the rate at which individuals recover from the disease. This balance ensures that the number of infected individuals remains constant at zero [28].

• Stability: Whether DFE is stable or unstable depends on the specific disease and the parameters of the model. A stable DFE means that if the number of infected individuals deviates slightly from zero, it will eventually return to zero. Conversely, an unstable DFE means that any small deviation from zero will lead to an outbreak of the disease [28].

The DFE of model in equation (2) is obtained by setting the RHS of system (2) equal to zero.

$$\left. \begin{aligned} \Lambda - \pi_1 S_c^o p - (\theta + \mu_1) S_c^o &= 0, \\ \theta S_c^o - (p\pi_2 + \alpha + \mu_1) S_m^o &= 0, \\ \alpha S_m^o - (\mu_1 + \eta) S_r^o &= 0, \\ (S_c^o \pi_1 + S_m^o \pi_2) P^o - (\omega_1 + \gamma + \mu_1) E^o &= 0, \\ \gamma E^o - (\delta + \mu_1 + \phi) I^o &= 0, \\ -\mu_1 R^o + \delta I^o + \eta S_r^o &= 0, \\ \omega_1 E^o + \omega_2 I^o - \mu_2 P^o &= 0. \end{aligned} \right\} \quad (14)$$

In the absence of disease, let  $I^o = E^o = P^o = 0$ , solving (14) gives

$$S_c^o = \frac{\Lambda}{\theta + \mu_1},$$

$$S_m^o = \frac{\theta \Lambda}{(\alpha + \mu_1)(\theta + \mu_1)},$$

$$S_r^o = \frac{\alpha \theta \Lambda}{(\alpha + \mu_1)(\theta + \mu_1)(\mu_1 + \eta)},$$

$$R^o = \frac{\eta \alpha \theta \Lambda}{(\alpha + \mu_1)(\theta + \mu_1)(\mu_1 + \eta)\mu_1},$$

hence the DFE for model (2) is given as

$$E^o = (S_c^o, S_m^o, S_r^o, E^o, I^o, R^o, P^o)$$

$$= \left( \frac{\Lambda}{\theta + \mu_1}, \frac{\theta\Lambda}{(\alpha + \mu_1)(\theta + \mu_1)}, \frac{\alpha\theta\Lambda}{(\alpha + \mu_1)(\theta + \mu_1)(\mu_1 + \eta)}, 0, 0, \frac{\eta\alpha\theta\Lambda}{(\alpha + \mu_1)(\theta + \mu_1)(\mu_1 + \eta)\mu_1}, 0 \right). \quad (15)$$

## 4. Basic reproduction number

The basic reproduction number, also called the basic reproduction ratio or rate, is an epidemiological metric used to describe the contagiousness or transmissibility of infectious agents.

The basic reproduction number, often abbreviated as  $R_o$ , is a key concept in epidemiology. It's a measure of how contagious a disease is, a higher  $R_o$  means that each infected pod, on average, infects more pods, leading to a faster spread of the disease. Conversely, a lower  $R_o$  indicates that the disease is less contagious and will spread more slowly [29]. For instance, if a disease has an  $R_o$  of 3, then one infected person can be expected to transmit the disease to 3 other people on average.

$R_o$  greater than 1 indicates that the infection will spread exponentially. Conversely, an  $R_o$  less than 1 means that the infection will die out. The concept is instrumental in understanding the spread of infectious diseases and implementing control measures. Public health interventions like vaccination aim to bring down the  $R_o$  below 1 to stop the spread of a disease.

According to [29], factors affecting the basic reproduction number are :

- **infectiousness of the disease:** this refers to how easily a disease can be transmitted from one person to another.
- **duration of the infectious period:** the longer an infected person remains contagious, the higher the chance of transmission.
- **rate of contact between susceptible individuals and infected individuals:** this depends on various factors like population density, social mixing patterns, and hygiene practices.

**Definition 1**  $R_o$  is the average number of secondary infections caused by a single infected individual in a population that is entirely susceptible to the disease [29].

Computation of  $R_o$  is carried out using the next generation matrix as laid out in [29].  $R_o$  is obtained using

$$R_o = \rho(FV^{-1}), \quad (16)$$

where  $\rho$  is the spectral radius of the matrix  $FV^{-1}$ . Differential equations which is associated with  $E, I, P$  compartment are the infective classes and will be used in the computation of  $R_o$ .

$$\left. \begin{aligned} \frac{dE}{dt} &= (\pi_1 S_c + \pi_2 S_m)P - (\omega_1 + \gamma + \mu_1)E, \\ \frac{dI}{dt} &= \gamma E - (\delta + \mu_1 + \psi)I, \\ \frac{dP}{dt} &= \omega_1 E + \omega_2 I - \mu_2 P. \end{aligned} \right\} \quad (17)$$

From system (17), we derive

$$F_i = \begin{pmatrix} (\pi_1 S_c + \pi_2 S_m) P \\ 0 \\ 0 \end{pmatrix}, V_i = \begin{pmatrix} (\gamma + \mu_1) E \\ (\delta + \mu_1 + \phi) - \gamma E \\ \mu_2 P - \omega_1 E - \omega_2 I \end{pmatrix},$$

and it follows that

$$F = \begin{pmatrix} 0 & 0 & \frac{\pi_1 \Lambda}{(\theta + \mu_1)} + \frac{\pi_2 \theta \Lambda}{(\theta + \mu_1)(\alpha + \mu_1)} \\ 0 & 0 & 0 \\ 0 & 0 & 0 \end{pmatrix},$$

$$V = \begin{pmatrix} (\gamma + \mu_1) & 0 & 0 \\ -\gamma & (\delta + \mu_1 + \phi) & 0 \\ -\omega_1 & -\omega_2 & \mu_2 \end{pmatrix}.$$

$R_o$  which is the dominant eigenvalue of equation (16) is obtained as

$$R_o = \frac{(\pi_1 \Lambda (\alpha + \mu_1) + \pi_1 \theta \Lambda) (\gamma \omega_2 + \gamma \omega_1 + \omega_1 \mu_1)}{\mu_2 (\theta + \mu_1) (\alpha + \mu_1) (\gamma + \mu_1) (\delta + \mu_1 + \phi)}, \quad (18)$$

equation (18) is the basic reproduction number for model (2)

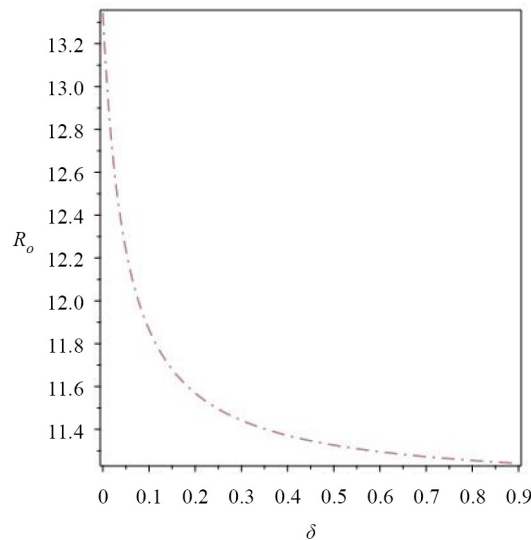


Figure 2. plot of  $R_o$  against  $\delta$

**Remark 1** (i) whenever  $R_o > 1$ , it indicates that each infected pod, on average, will infect more than one other person, leading to an outbreak or epidemic.

(ii) Whenever  $R_o < 1$ , it means that the disease will likely die out on its own, as each infected pod, on average, infects fewer than one other pod.

(iii) Whenever  $R_o = 1$ , it indicates new cases remains constant, neither increasing nor decreasing, the outbreak is not actively growing, but it's not dying out either.

Figure 2 is a plot of basic reproduction number against  $\delta$ , which is the transmission rate from  $I$  to  $R$ , the higher the rate of  $\alpha$ , the lower the  $R_o$ , thus effort must be geared toward the prevention of the infection.

#### 4.1 Existence and uniqueness of endemic equilibrium

Endemic Equilibrium (EE) state is the state where the disease persist.

Let

$$E^+ = (S^+c, S^+m, S^+r, E^+, I^+, R^+, P^+),$$

be the EE state. In order to obtain the EE state, equation (2) need to be rearrange and solve simultaneously, i.e

$$\begin{aligned} \Lambda - \pi_1 S_c^+ P^+ - (\theta + \mu_1) S_c^+ &= 0, \\ \theta S_c^+ - (P^+ \pi_2 + \alpha + \mu_1) S_m^+ &= 0, \\ \alpha S_m^+ - (\mu_1 + \eta) S_r^+ &= 0, \\ (S_c^+ \pi_1 + S_m^+ \pi_2) P^+ - (\omega_1 + \gamma + \mu_1) E^+ &= 0, \\ \gamma E^+ - (\delta + \mu_1 + \phi) I^+ &= 0, \\ -\mu_1 R^+ + \delta I^+ + \eta S_r^+ &= 0, \\ \omega_1 E^+ + \omega_2 I^+ - \mu_2 P^+ &= 0, \end{aligned} \tag{19}$$

if

$$R_o = \frac{(\pi_1 \Lambda (\alpha + \mu_1) + \pi_1 \theta \Lambda) (\gamma \omega_2 + \gamma \omega_1 + \omega_1 \mu_1)}{\mu_2 (\theta + \mu_1) (\alpha + \mu_1) (\gamma + \mu_1) (\delta + \mu_1 + \phi)},$$

then

$$S^+ = \frac{S^o}{R_o}, \tag{20}$$

therefore

$$S^+ = \frac{\Lambda}{(\theta + \mu_1)R_o}. \quad (21)$$

Substitute (21) into the first equation of system (19)

$$\Lambda - \frac{\pi_1 P^+ \Lambda}{(\theta + \mu_1)R_o} - \frac{(\theta + \mu_1)\Lambda}{(\theta + \mu_1)R_o} = 0$$

thus, solving for  $P^+$  gives

$$P^+ = \frac{(\theta + \mu_1)(R_o - 1)}{\pi_1}. \quad (22)$$

Substitute (21) and (22) into the second equation of (19) and simplify

$$S_m^+ = \frac{\theta \Lambda \pi_1}{(\theta + \mu_1)R_o [\pi_2(\theta + \mu_1)(R_o - 1) + \pi_1(\alpha + \mu_1)]}. \quad (23)$$

Substitute (23) into the third equation of system (19), after simplification, we have

$$S_r^+ = \frac{\alpha \theta \Lambda \pi_1}{(\mu_1 + \eta)(\theta + \mu_1)R_o ((\theta + \mu_1)(R_o - 1) + \pi_1(\alpha + \mu_1))}. \quad (24)$$

From equation (5) of the system (19)

$$E^+ = \frac{(\delta + \mu_1 + \psi)}{\gamma} I^+. \quad (25)$$

Substitute (25) into the seventh equation of system (19),

$$\omega_1 \frac{(\delta + \mu_1 + \psi)}{\gamma} I^+ + \omega_2 I^+ + \mu_2 P^+ = 0,$$

$$I^+ = \frac{\mu_2 P^+ \gamma}{\pi_1(\omega_1(\delta + \mu_1 + \psi) + \omega_2 \gamma)}.$$

Inserting  $P^+$  into the above, gives

$$I^+ = \frac{\mu_2 \gamma (\theta + \mu_1)}{\pi_1(\omega_1(\delta + \mu_1 + \psi) + \omega_2 \gamma)}, \quad (26)$$

substitute (26) into (25) and simplify

$$E^+ = \frac{\mu_2(\theta + \mu_1)(\delta + \mu_1 + \psi)(R_o - 1)}{\pi_1(\omega_1(\delta + \mu_1 + \psi) + \omega_2\gamma)}. \quad (27)$$

From equation (7) of the system (19)

$$R^+ = \frac{\delta I^+}{\mu_1} + \frac{\eta S_r^+}{\mu_1}, \quad (28)$$

substitute the values of  $S_r^+$  &  $I^+$  into (28) gives

$$R^+ = \frac{C}{W}, \quad (29)$$

where  $C = \delta\mu_2\gamma(\theta + \mu_1)(R_o - 1)(\theta + \mu_1)R_o(\pi_2(\theta + \mu_1)(R_o - 1) + \pi(\alpha + \mu_1)) + \alpha\eta\theta\Lambda\pi_1^2(\omega_1(\delta + \mu_1 + \psi) + \omega_2\gamma)$  and  $W = \mu_1\pi_1[(\omega_1(\delta + \mu_1 + \psi) + \omega_2\gamma)(\mu_1 + \eta)(\theta + \mu_1)R_o] + \pi_2(\theta + \mu_1)(R_o - 1) + \pi_1(\alpha + \mu_1)$

The existence of an endemic equilibrium often depends on the basic reproduction number ( $R_o$ ).

- If  $R_o$  is less than 1 ( $R_o < 1$ ), the disease cannot establish itself in the population, and the disease-free equilibrium is stable. The infection will eventually die out. If  $R_o$  is greater than 1 ( $R_o > 1$ ), an endemic equilibrium typically exists. The infection persists in the population, and the number of infected individuals stays relatively constant over time.

## 5. Stability analysis

### 5.1 Local stability of disease free equilibrium

Local stability analysis is a mathematical technique used to investigate the behavior of a system around an equilibrium point. It's particularly useful in understanding how a system responds to small disturbances.

**Theorem 1** The disease free equilibrium of model (2) is locally asymptotically stable If  $\mathfrak{R}_o < 1$ , otherwise, it is unstable.

**Proof.** The Jacobian matrix  $J$  of model (2) will be computed by differentiating each equation in system with respect to state variables  $S_c, S_m, S_r, E, I, R, P$ . The model system (2) linearized around the DFE solution (15) yields the Jacobian matrix below:

$$J(E^o) = \begin{pmatrix} -(\theta + \mu_1) & 0 & 0 & 0 & 0 & 0 & -\pi_1 \\ 0 & -(\alpha + \mu_1) & 0 & 0 & 0 & 0 & -\pi_2 \\ 0 & \alpha & -(\mu_1 + \eta) & 0 & 0 & 0 & 0 \\ 0 & 0 & 0 & -(\gamma + \mu_1) & 0 & 0 & \pi_1 + \pi_2 \\ 0 & 0 & 0 & \gamma & -(\delta + \mu_1 + \psi) & 0 & 0 \\ 0 & 0 & \eta & 0 & \delta & -m\mu_1 & 0 \\ 0 & 0 & 0 & \omega_1 & \omega_2 & 0 & -\mu_2 \end{pmatrix}, \quad (30)$$

we use the trace and determinant of matrix to ascertain the stability of model (2).

The trace of matrix ( $J^o$ ) is obtained as

$$\begin{aligned} \text{tr}(J^o) &= -\theta - 6\mu_1 - \alpha - \eta - \gamma - \delta - \psi - \mu_2 \\ &= -(\theta + 6\mu_1 + \alpha + \eta + \gamma + \delta + \psi + \mu_2) \end{aligned}$$

Therefore,  $\text{tr}(J^o) < 0$ .

Likewise, the determinant of matrix  $(J^o)$  in equation (30) is given as

$$\det(J^o) = [p_3 (\omega_1 (\delta + \mu_1 + \psi) + \gamma\omega_2) - \mu_2 (\gamma + \mu_1) (\delta + \omega_1 + \psi)] (\theta + \mu_1) (\alpha + \mu_1) (\mu_1 + \eta) \mu_1,$$

where  $p_3 = \pi_1 + \pi_2$ , □

$$\det \geq 0, \text{ iff } p_3 (\omega_1 (\delta + \mu_1 + \psi) + \gamma\omega_2) > \mu_2 (\gamma + \mu_1) (\delta + \omega_1 + \psi).$$

## 5.2 Global stability of disease free equilibrium point

**Theorem 2** The disease-free equilibrium point  $E^o$  tends to remain globally asymptotically stable if  $\mathfrak{R}_0 \leq 1$ , otherwise unstable.

**Proof.** Details of how to proof Theorem 2 can be found in [24]. □

## 6. Sensitivity analysis

Sensitivity analysis is a powerful tool used to understand how changes in input variables affect the output of a model or system. Its benefit includes [30]:

- (i) improves decision-making: providing insights into risk and uncertainty;
- (ii) builds confidence in models and forecasts; understanding how your predictions react to different scenarios makes them more reliable;
- (iii) identifies critical factors to focus on and
- (iv) helps to optimize resource allocation and planning.

**Definition 2** The below formula is used to describe the standardized forward sensitivity index of a variable C that differently relies on a parameter  $s$ , see [31, 32] for more details.

$$Z_s^C = \frac{\partial C}{\partial s} \times \frac{s}{C}. \quad (31)$$

The sensitivity indices of reproduction number  $\mathfrak{R}_o$  corresponding to our model parameters is described below

$$M_{\pi_1}^{R_o} = \frac{\partial R_o}{\partial \pi_1} \times \frac{\pi_1}{R_o} = +0.95238095. \quad (32)$$

In a similar way, remaining indices for the model parameters are obtained and displayed in Table 2.

**Table 2.** sensitivity indices of  $\mathfrak{R}_0$

Parameters	Sensitivity indices
$\pi_1$	+0.952380951
$\pi_2$	+0.047619048
$\Lambda$	+1.000000000
$\alpha$	- 0.023414027
$\mu_1$	-1.333004883
$\mu_2$	-1.000000000
$\theta$	-0.428571421
$\omega_1$	+0.933377748
$\omega_2$	+0.066622252
$\gamma$	-0.100044415
$\delta$	-0.042798044
$\psi$	-0.000047555

The value with negative indices is an important parameter employed in the control of the disease because the value of  $R_0$  grows when the index with a positive indication is increased and decreases when the index with a negative indication is increased.

## 7. Analysis of optimal control

Optimal control theory takes epidemic modeling a step further. It allows us to actively guide the course of an outbreak by finding the best possible control strategies to achieve a desired outcome. It helps to steer the course of outbreaks towards favorable outcomes. Pontryagin's Maximum Principle [33], which has been widely used in mathematical models of biological processes including optimal control, serves as the foundation for the study. The optimal control in this paper focuses on:

- $u_1$ : Good sanitation, weed control and pruning
- $u_2$ : Treatment effort on the infected pods, they include using an appropriate fungicides.
- $u_3$ : Pod removal (Rouging).

The following goal or cost-functional approach is used to reduce the populations of Pathogen ( $P(t)$ ) in pod exposure and infection, while also reducing the expenses associated with putting the control strategies  $u_i(t)$  ( $i = 1, 2, 3$ ) into action:

$$J = \int_0^T \left( W_1 S_c(t) + W_2 S_m(t) + W_3 I(t) + \frac{1}{2} \sum_{i=1}^3 B_i u_i^2(t) \right) dt, \quad (33)$$

subject to model in equation (2), where  $W_1, W_2, W_3$  and  $B_i, i = 1, 2, 3$  are positive weight constants.  $T$  is a representation of the anticipated completion time for the controls implementation.

The cost control function for fungicide application  $\frac{1}{2} B_2 u_2^2$ , the cost of practicing excellent sanitation  $\frac{1}{2} B_1 u_1^2$ , and the cost of rouging (pod removal)  $\frac{1}{2} B_3 u_3^2$  are all included in the objective functional in equation (33). Similar to previous research [13, 34–36], the cost control functions in this study adopt a quadratic form.

In order to achieve our set objectives, we seek an optimal control triple,  $u^* = (u_i^*), i = 1, 2, 3$ , such that

$$J(u^*) = \min \{J(u_1, u_2, u_3 | u_i \in U)\}, \quad (34)$$

where  $U = \{u_i(t): 0 \leq u_i(t) \leq 1, \text{ Lebesgue measurable, } t \in [0, T]\}$  which is a non empty control set.

### 7.1 Characterization of the optimal control

In order to obtain the necessary conditions for optimal control of cocoa black pod disease, which is governed by the non-autonomous system in equation (2), we make use of the Pontryagin's Maximum Principle [33], which converts the state system (2), together with the objective functional (33) and (34) into a problem of minimizing pointwise, with respect to the controls  $u_1, u_2$ , and  $u_3$ , a Hamiltonian  $H$  given by :

$$\begin{aligned}
 H = & W_1 S_c + W_2 S_m + W_3 I + \lambda_1 [\Lambda - \pi_1 P S_c - (\theta + \mu_1 + u_1) S_c] + \lambda_2 [\theta S_c - (\pi_2 P + \alpha + \mu_1 + u_2) S_m] \\
 & + \lambda_5 [\gamma E - (\delta + \mu_1 + \psi + u_3) I] + \lambda_3 [\alpha S_m - (\mu_1 + \eta) S_r] \\
 & + \lambda_4 [(\pi_1 S_c + \pi_2 S_m) P - (\omega_1 + \gamma + \mu_1) E + u_1 S_c + u_2 S_m] \\
 & + \lambda_5 [\gamma E - (\delta + \mu_1 + \psi + u_3) I] + \lambda_6 [\delta I + u_3 I + \eta S_r - \mu_1 R] + \lambda_7 [\omega_1 E + \omega_2 I - \mu_2 P], \quad (35)
 \end{aligned}$$

where  $\lambda_1, \lambda_2, \lambda_3, \lambda_4, \lambda_5, \lambda_6$  and  $\lambda_7$  are the adjoint variables. The requisite conditions for the ideal control are provided by the following lemma.

**Lemma 3** Considering an optimal control triple  $(u_1^*, u_2^*, u_3^*)$  that minimizes objective functional (21) over the control set  $U$  subject to the state system (2), then there exist adjoint variables  $\lambda_1, \lambda_2, \lambda_3, \lambda_4, \lambda_5, \lambda_6, \lambda_7$  satisfying

$$\left. \begin{aligned}
 \frac{dS_c}{dt} &= \Lambda - \pi_1 P S_c - (\theta + \mu_1 + u_1) S_c, \\
 \frac{dS_m}{dt} &= \theta S_c - (\pi_2 P + \alpha + \mu_1 + u_2) S_m, \\
 \frac{dS_r}{dt} &= \alpha S_m - (\mu_1 + \eta) S_r, \\
 \frac{dE}{dt} &= (\pi_1 S_c + \pi_2 S_m) P - (\omega_1 + \gamma + \mu_1) E + u_1 S_c + u_2 S_m, \\
 \frac{dI}{dt} &= \gamma E - (\delta + \mu_1 + \psi + u_3) I, \\
 \frac{dR}{dt} &= \delta I + u_3 I + \eta S_r - \mu_1 R, \\
 \frac{dP}{dt} &= \omega_1 E + \omega_2 I - \mu_2 P,
 \end{aligned} \right\} \quad (36)$$

coupled with the transversality conditions

$$\lambda_1(T) = 0, \lambda_2(T) = 0, \lambda_3(T) = 0, \lambda_4(T) = 0, \lambda_5(T) = 0, \lambda_6(T) = 0, \lambda_7(T) = 0, \quad (37)$$

and

$$\begin{aligned} u_1(t) &= \min \left\{ \max \left( 0, \frac{(\lambda_1 - \lambda_4)}{B_1} S_c \right), 1 \right\}, \\ u_2(t) &= \min \left\{ \max \left( 0, \frac{(\lambda_2 - \lambda_4)}{B_2} S_m \right), 1 \right\}, \\ u_3(t) &= \min \left\{ \max \left( 0, \frac{(\lambda_5 - \lambda_6)}{B_3} I \right), 1 \right\}. \end{aligned} \quad (38)$$

**Proof.** By obtaining partial derivatives of the Hamiltonian  $H$  given by (35) with respect to the corresponding state variables, the adjoint equations defined by the non-autonomous system (36) are derived.

$$\begin{aligned} \frac{d\lambda_1}{dt} &= -\frac{\partial H}{\partial S_c}, & \frac{d\lambda_2}{dt} &= -\frac{\partial H}{\partial S_m}, & \frac{d\lambda_3}{dt} &= -\frac{\partial H}{\partial S_r} \\ \frac{d\lambda_4}{dt} &= -\frac{\partial H}{\partial E}, & \frac{d\lambda_5}{dt} &= -\frac{\partial H}{\partial I}, & \frac{d\lambda_6}{dt} &= -\frac{\partial H}{\partial R}, & \frac{d\lambda_7}{dt} &= -\frac{\partial H}{\partial P}, \end{aligned}$$

with transversality conditions (37). Also, the optimal control characterization given by (35) is determined by solving the following partial differential equations:

$$\frac{\partial H}{\partial u_1} = 0 \text{ for } u_1^*,$$

$$\frac{\partial H}{\partial u_2} = 0 \text{ for } u_2^*,$$

$$\frac{\partial H}{\partial u_3} = 0 \text{ for } u_3^*.$$

Therefore, using standard control arguments involving control boundaries,

$$u_i^* = \begin{cases} 0, & \text{if } u_i^* \leq 0, \\ u_i^*, & \text{if } 0 \leq u_i^* \leq 1, \\ 1, & \text{if } u_i^* \geq 1, \end{cases} \quad (39)$$

for  $i = 1, 2, 3$  and

$$u_1^* = \frac{(\lambda_1 - \lambda_4)}{B_1} S_c,$$

$$u_2^* = \frac{(\lambda_2 - \lambda_4)}{B_2} S_m,$$

$$u_3^* = \frac{(\lambda_5 - \lambda_6)}{B_3} I.$$

□

## 8. Numerical simulation and discussion of results

The state equations (2) along with the adjoint equations (36) containing the starting points at  $t = 0$ , as well as the final conditions (37) and the characterization of the optimum control (38), make up the 14-dimensional the optimal state system. Using an iterative sweep method and a fourth-order forward-backward Runge-Kutta scheme, this optimality system is solved. Using an initial guess for the controls across the simulated time, the state equations (2) are solved forward in time, because of the terminal conditions, the adjoint system is solved backward in time using the state equations' current iteration respond to (36) (see [37] for more details on the numerical procedure).

To illustrate the impact of different optimal control intervention strategies on the transmission of black pod in a pod population, the following control measures to curtail the transmission of cocoa black pod disease are considered.

- (i) Strategy 1: Using  $u_1 = 0, u_2 = 0, u_3 = 0$ ,
- (ii) Strategy 2: Using  $u_1 = 0, u_2 \neq 0, u_3 \neq 0$ ,
- (iii) Strategy 3: Using  $u_1 \neq 0, u_2 = 0, u_3 \neq 0$ ,
- (iv) Strategy 4: Using  $u_1 \neq 0, u_2 \neq 0, u_3 = 0$ ,
- (v) Strategy 5: Using  $u_1 = 0, u_2 = 0, u_3 \neq 0$ ,
- (vi) Strategy 6: Using  $u_1 \neq 0, u_2 = 0, u_3 = 0$ ,
- (vii) Strategy 7: Using  $u_1 = 0, u_2 \neq 0, u_3 = 0$ ,
- (viii) Strategy 8: Using  $u_1 \neq 0, u_2 \neq 0, u_3 \neq 0$ .

The parameter values from Table 1 are used such that  $R_0 = 11.91825458$  with initial conditions  $S_c(0) = 1500, S_m(0) = 0, S_r(0) = 0, E(0) = 0, I(0) = 0, R(0) = 0$  and  $P(0) = 30$ . The weight constants values are carefully chosen such that  $B_1 = 30, B_2 = 30, B_3 = 30, W_1 = 20, W_2 = 20, W_3 = 20$ . The choice of the initial conditions were based on mere ecological observation. Likewise, finding the optimal weight values can be an iterative process, and there may not be a single "correct" answer, the goal is to choose weights that lead to a solution that best reflects the desired trade-offs and priorities of the specific optimal control problem. The maximum value of  $u$  was considered ( $0 \leq u \leq 1$ ), this is necessary to attain a optimal result.

We will delve into the key results presented in Figure 3 to 17. The research intends to determine the impact of optimal control on the transmission of cocoa black pod disease, i e. to control the rate of transmission from the infected pods to the susceptible pods. The control is applied in 90 days which implies that the final time  $T = 90$ . The simulations were carried out using the values taken from the literature, as presented in Table 1 and with the use of MATLAB software.

Serving as the foundation of this study, Figures 3-9 depict the impact of various optimal control interventions on cocoa black pod disease transmission dynamics.

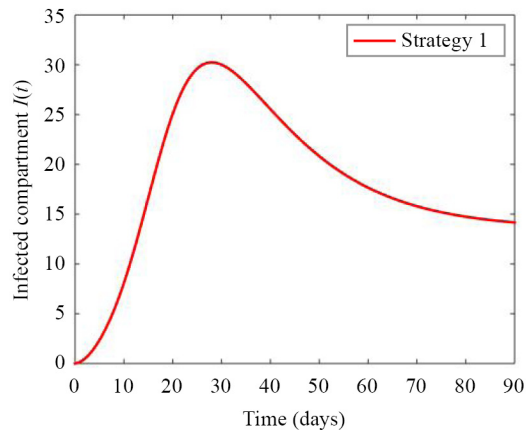


**Figure 3.** Plot of control strategy 1 against the infected compartment

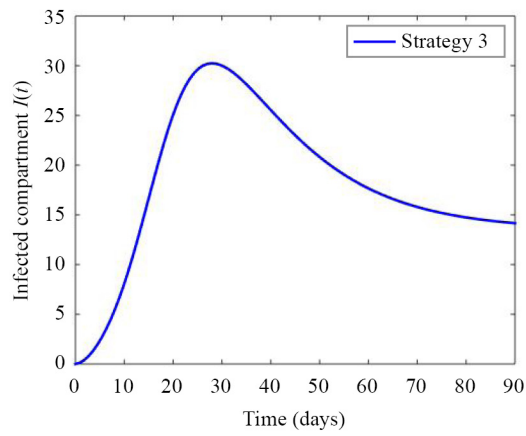


**Figure 4.** Plot of control strategy 3 against the infected compartment

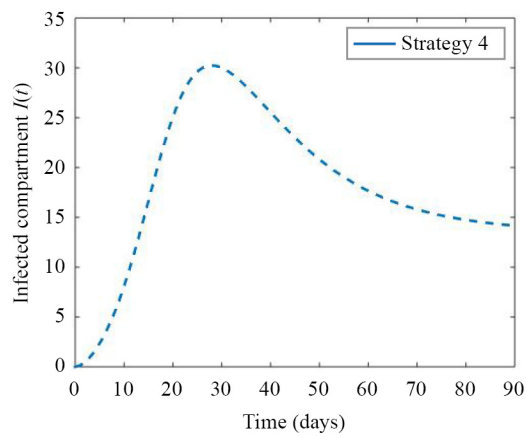


**Figure 5.** Plot of control strategy 4 against the infected compartment

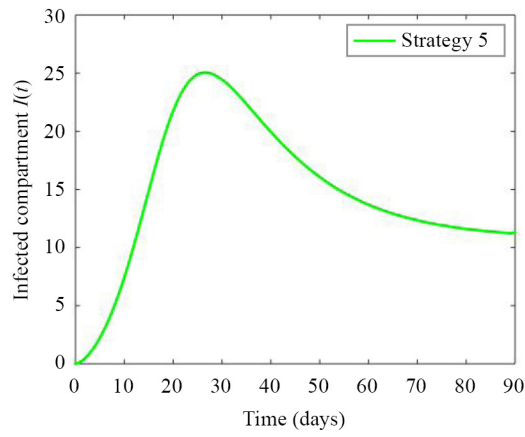


**Figure 6.** Plot of control strategy 5 against the infected compartment

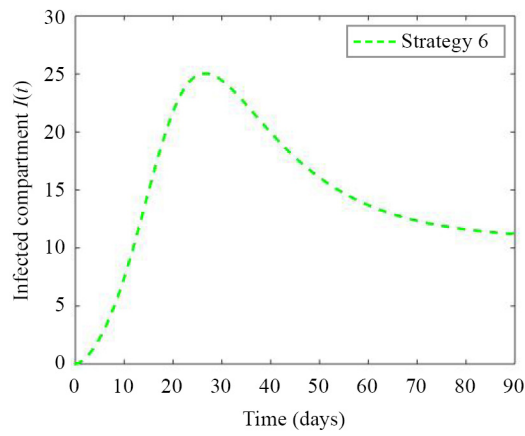


**Figure 7.** Plot of control strategy 6 against the infected compartment

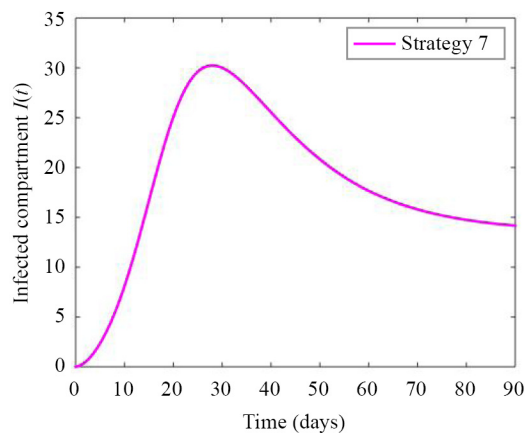


**Figure 8.** Plot of control strategy 7 against the infected compartment

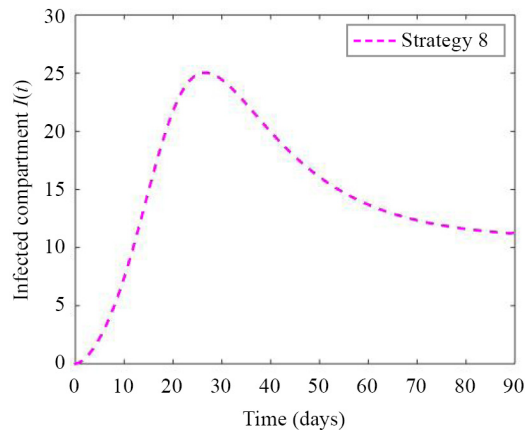


**Figure 9.** Plot of control strategy 8 against the infected compartment

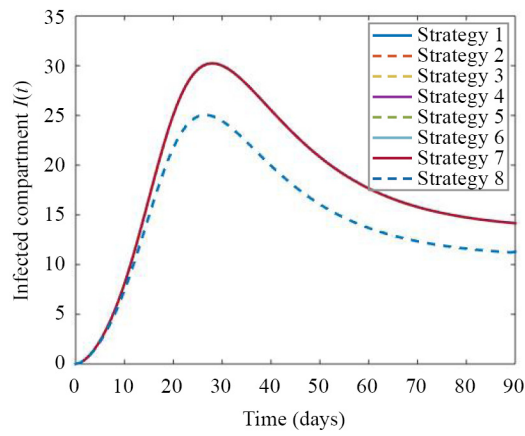


**Figure 10.** Combined control strategies to curtail the disease spread

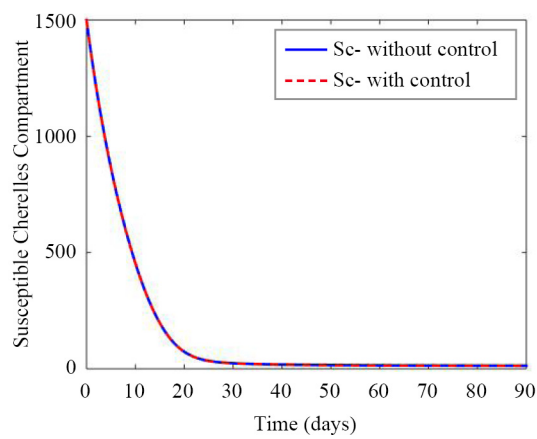


**Figure 11.** Cherelles against time

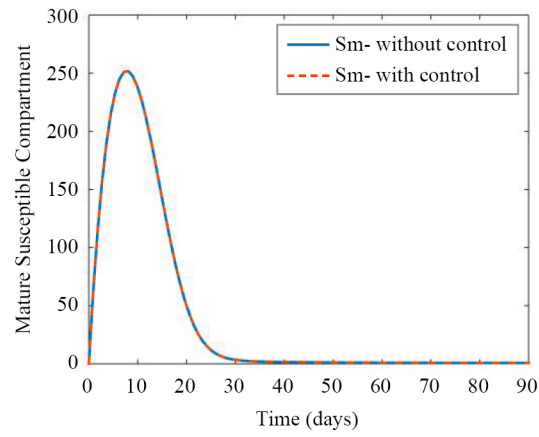


**Figure 12.** Young and mature pods against time

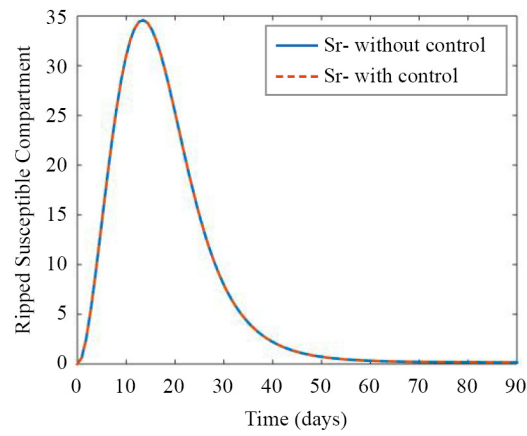


**Figure 13.** Ripe pods against time

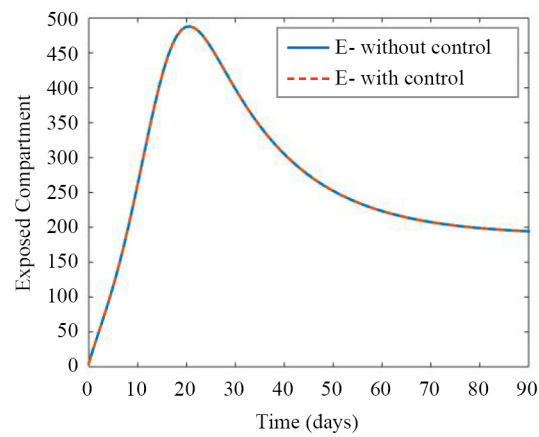


**Figure 14.** Exposed pods against time

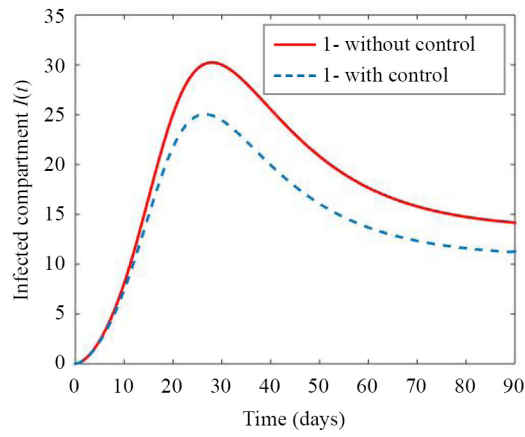


Figure 15. Infected pods against time

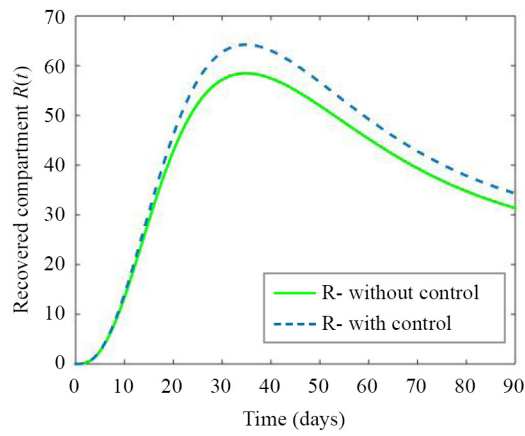


Figure 16. Removed pods against time

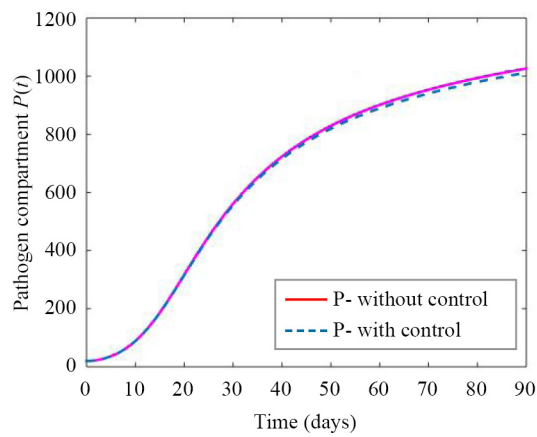


Figure 17. Pathogens against time

Figure 10 represents the effect of the 8 control strategies on the infected pods, strategy 2, strategy 3, strategy 5 and strategy 8 has a reduced number of infected pods when compared with strategy 1, strategy 4, strategy 6 and strategy 7 as reveal by the plot, this signifies that strategy 2, strategy 3, strategy 5 and strategy 8 are more effective in the control of the disease, The study recommends that control measure  $u_3$  which is rouging (pod removal) and any one of the remaining control measures for the treatment of cocoa black pod disease caused by *Phytophthora Megarkaya*.

Figure 11 presents the plot of Cherelles compartment ( $S_c$ ) against time with and without control measures, the plot signifies no significant effect with the application of control measures on the Cherelles compartment.

Figure 12 presents the plot of young and mature pod compartment ( $S_p$ ) against time with and without control measures, the plot signifies no significant effect with the application of control measures.

Figure 13 presents the plot of ripe pods compartment ( $S_r$ ) against time with and without control measures, the plot signifies no significant effect with the application of control measures.

Figure 14 presents the plot of exposed pod compartment  $E$  against time with and without control measures, the plot signifies no significant effect with the application of control measures.

Figure 15 presents the plot of infected pod compartment ( $I$ ) with and without control measures, the plot reveals a significant effect with the application of control measures on the effected pod compartment, thus signifies the effectiveness of the control measure applied.

Figure 16 presents the plot of removed pod (harvested) compartment with and without control measures, number of harvested pods increases significantly due to the control measure applied.

Figure 17 presents the plot of the Pathogen compartment  $P$  with and without control measures, there is a little significant effect with the application of control measures.

## 9. Conclusion

This study investigated the application of mathematical modeling and optimal control strategies to cocoa black pod disease, caused by the fungal pathogen *Phytophthora megakarya*. We developed a mathematical model that captures the key dynamics of the disease cycle. Using optimal control theory, we explored various control strategies to minimize disease prevalence and mitigate pod losses.

Our simulations as illustrated in Figures 3-17 demonstrated that optimal control strategies can significantly reduce cocoa black pod transmission compared to uncontrolled scenarios. The results highlight the potential of pod removal, fungicide application and sanitation practices to effectively manage the disease as supported by the findings of [7, 14, 20, 24].

Furthermore, the sensitivity analysis revealed factors critical for successful disease control. This information is valuable for tailoring intervention strategies to specific growing regions and farm practices.

In conclusion, this study presented a mathematical framework for analyzing and controlling cocoa black pod disease. The findings advocate for the integration of optimal control approaches into integrated disease management programs for cocoa production. Future research could explore the economic viability of these strategies and investigate their broader application across diverse farming landscapes.

## Acknowledgement

The authors wish to thank the anonymous referees for their careful reading of the manuscript and their fruitful comments and suggestions.

## Conflict of interest

The authors declare no competing financial interest.

## References

- [1] Abiodun O, Olukayode A, Ndako J. Mathematical Modeling and Its Methodological Approach: Application to Infectious Disease. *2023 International Conference on Science, Engineering and Business for Sustainable Development Goals (SEB-SDG)*. Omu-Aran, Nigeria; 2023. p.1-14. Available from: <https://doi.org/10.1109/SEB-SDG57117.2023.10124470>.
- [2] Mata AS, Dourado SMP. Mathematical modeling applied to epidemics: An overview. *Paulo Journal of Mathematical Sciences*. 2021; 15: 1025-1041.
- [3] Naidoo M, Shephard W, Kambewe I. Incorporating social vulnerability in infectious disease mathematical modelling: A scoping review. *BMC Medicine*. 2024; 22: 125-158.
- [4] Phytophthora megakarya on Wikipedia. 2024. Available from: <https://en.wikipedia.org/wiki/Phytophthora>.
- [5] Junaid M, Gassa A, Rosmana A, Bakar S. First report of Phytophthora black pod disease of cocoa spread by Iridomyrmex cordatus in Sulawesi: A dilemma about predatory insect for cocoa pest control. *IOP Conference Series: Earth and Environmental Science*. 2020; 486(1): 012169. Available from: <https://dx.doi.org/10.1088/1755-1315/486/1/012169>.
- [6] Ali S, Shao J, Lary D, Strem M, Meinhardt L, Bailey B. Phytophthora megakarya and P. palmivora, causal agents of black pod rot, induce similar plant defense responses late during infection of susceptible cacao pods. *Frontiers in Plant Science*. 2017; 8: 169.
- [7] Afoakwa EO. *Cocoa Production and Processing Technology*. USA: CRC Press, Taylor and Francis Group; 2014.
- [8] Akem TM, Adebayo OA. Modelling and control of fungal diseases of cocoa: A review. *Journal of Applied Mathematics and Statistics*. 2013; 2(2): 15-23.
- [9] Food and Agriculture Organization of the United Nations. How to Feed the World in 2050: Highlighting the need for food and agriculture transformation. 2019. Available from: <https://www.fao.org/fileadmin/templates/wsfs/docs/expertpaper/HowtoFeedtheWorldin2050.pdf>.
- [10] Gilligan CA, Van der Ploeg RR. Including spatial patterns in epidemiological models of crop diseases. A review. *Agricultural and Forest Meteorology*. 2014; 198-199: 1-13.
- [11] Baudron F. Age-structured models for plant disease spread: The case of Septoria tritici blotch on wheat. *Phytopathology*. 2018; 108(7): 853-863.
- [12] Madden LV, Hughes G, van der Plank RE. *The study of plant disease epidemics*. APS Press; 2017.
- [13] Hugo A, Makinde OD, Kumar S, Chibwana FF. Optimal control and cost effectiveness analysis for Newcastle disease eco-epidemiological model in Tanzania. *Journal of Biological Dynamics*. 2017; 11(1): 190-209.
- [14] Adeniran A, Onanaye A, Adeleke O. Optimal control of Cocoa Black pod disease: A multipronged approach. *Franklin Open*. 2024; 7: 100100. Available from: <https://doi.org/10.1016/j.fraope.2024.100100>.
- [15] Kouamou J, Mboup M. Optimal control of black pod disease in cocoa plantations: A dynamic programming approach. *Journal of Mathematical Biology*. 2012; 65(5): 875-894.
- [16] Tonny AC. Optimal control model and cost effectiveness analysis of maize streak virus pathogen interaction with pest invasion in maize plant. *Biotechnology Letters*. 2020; 42(4): 881-892.
- [17] Zhao XQ, Xiao D. Optimal control of a stochastic plant virus propagation model with impulsive toxicant input. *Journal of Mathematical Analysis and Applications*. 2013; 405(2): 507-523.
- [18] Derycke V, Jabbour H. Modelling and optimal control of black pod disease of cocoa. *Ecological Modeling*. 2013; 221(10-13): 1209-1215.
- [19] Gottwald TR, Mundt CM. A mathematical model for the spread of cacao black pod disease. *Phytopathology*. 1982; 72(12): 1271-1278.
- [20] N'Guessan KA, Kouassi AM, Ahipo AG. Development and application of a stochastic model for the control of black pod disease in cocoa plantations in Côte d'Ivoire. *International Journal of Biometeorology*. 2013; 57(7): 1161-1173.
- [21] Ollennu LAA, Owusu GK. Spread of cocoa swollen shoot virus to cacao (*Theobroma cacao* L.) plantings in Ghana. *Tropical Agriculture*. 2002; 79(4): 224-230.
- [22] Zhang C, Dong Y, Li Tang T, Yi Zheng D, Makowski G, Yang Yu F, et al. Intercropping cereals with faba bean reduces plant disease incidence regardless of fertilizer input; a meta-analysis. *European Journal of Plant Pathology*. 2019; 154: 931-942.
- [23] Kouamou W, Mboup M. Optimal control of plant diseases: A review. *Phytopathology*. 2017; 107(10): 1287-1302.

- [24] Adeniran A, Onanaye A, Adeleke O. Mathematical model for spread and control of cocoa black pod disease. *Contemporary Mathematics*. 2023; 4(3): 549-568.
- [25] Bisselua D, Yede D, Vidal S. Dispersion models and sampling of cacao mirid bug *Sahlbergella singularis* (hemiptera: Miridae) on *Theobroma cacao* in southern Cameroon. *Environmental Entomology*. 2011; 10: 111-119.
- [26] Nyaberi HO, Mutuku WN, Malonza DM, Gachigua GW. A Mathematical model of the dynamics of Coffee Berry Disease. *Journal of Applied Mathematics*. 2023; 2023: 9320795. Available from: <https://doi.org/10.1155/2023/9320795>.
- [27] Takam Soh E, Ndong Nguema P, Gwet H, Ndoumbe-Nkeng M. Smooth estimation of a lifetime distribution with competing risks by using regular interval observations: Application to cocoa fruits growth. *Applied Statistics*. 2013; 62: 741-760.
- [28] Brauer F. Mathematical epidemiology: Past, present, and future. *Infectious Disease Modelling*. 2017; 2: 113-127.
- [29] Van den Driessche P, Watmough J. Reproduction numbers and sub-threshold endemic equilibria for compartmental models of disease transmission. *Mathematical Biosciences*. 2002; 180: 29-48.
- [30] Akingbade JA, Ogundare BS. Boundedness and stability properties of solutions of mathematical model of measles. *Tamkang Journal of Mathematics*. 2021; 51(1): 91-112.
- [31] Adedeji-Adenola H, Olugbake OA, Adeosun SA. Factors influencing COVID-19 vaccine uptake among adults in Nigeria. *PLoS ONE*. 2022; 17(2): e0264371. Available from: <https://doi.org/10.1371/journal.pone.0264371>.
- [32] Chitnis N, Hyman JM, Cushing JM. Determining important parameters in the spread of malaria through the sensitivity analysis of a mathematical model. *Bulletin of Mathematical Biology*. 2008; 70: 1272-1296.
- [33] Pontryagin LS, Boltyanskii VG, Gamkrelidze RV, Mishchenko EF. *The Mathematical Theory of Optimal Processes*. New York: Wiley; 1962.
- [34] Gervas E, Opoku NK, Ibrahim S. Mathematical modelling of human African trypanosomiasis using control measures. *Computational and Mathematical Methods in Medicine*. 2018; 2018: 113.
- [35] Modnak C. Mathematical modeling of an avian influenza: Optimal control study for intervention strategies. *Applied Mathematics & Information Sciences*. 2017; 11(4): 1049-1057.
- [36] Oke SI, Matadi MB, Xulu SS. Optimal control analysis of a mathematical model for breast cancer. *Mathematics and Computers in Simulation*. 2018; 23(21): 128.
- [37] Lenhart S, Workman JT. *Optimal Control Applied to Biological Models*. London: Chapman & Hall; 2007.